

Electronic Supplementary Information

**Sequestration of Acrylamide as Amino Acid-Acrylamide Adducts Mitigates Cellular Stress
in Human Gastrointestinal Cell Lines**

Axita Patel¹ and Bhaskar Datta^{1, 2*}

¹Department of Biological Sciences and Engineering, Indian Institute of Technology Gandhinagar,
Gandhinagar, Gujarat, India

²Department of Chemistry, Indian Institute of Technology Gandhinagar, Gandhinagar, Gujarat,
India

*Corresponding author

Table S1. Optimised reaction conditions needed for acrylamide-amino acid adduct formation. The reaction time was set for 120 mins for all four amino acids.

Compound	Temperature	pH	Amino acid concentration
Lysine Adduct	120 °C	7	50
Cysteine Adduct	120 °C	8	60
Glycine Adduct	80 °C	7	40
Methionine Adduct	120 °C	7	50

Table S2. Data for semi-preparative HPLC for the AA-ACR adducts.

Compound Name	Retention Time (mins)	Area (arbitrary units)	Concentration (arbitrary units)
Lys-ACR	5.664 5.919 6.238 12.304	1081 6484 2540207 345225	0.037 0.224 87.805 11.933
Gly-ACR	1.822 6.295 7.752 12.260	322341 3333583 210150 182110	7.963 82.348 5.191 4.499
Cys-ACR	6.138 6.747	70942 1174477	5.816 94.184
Met-ACR	10.126 12.00	12058995 592995	95.313 4.687

Based on comparative HPLC profiles of the individual amino acids and ACR, and validation by mass spectrometry, the peaks with retention times at 6.238 min, 6.295 min, 6.747 min and 10.126 min were attributed to the AA-ACR and were collected for subsequent work.

Table S3. Standard calibration plots for amino acid-acrylamide adducts.

Adducts	Linear equation	Regression coefficients (R ²)
Lys-ACR	$Y = 18034500x - 84210.0$	0.996
Gly-ACR	$Y = 31234000x + 12876.5$	0.998
Cys-ACR	$Y = 26795000x + 11340.3$	0.999
Met-ACR	$Y = 16589200x + 52378.9$	0.997

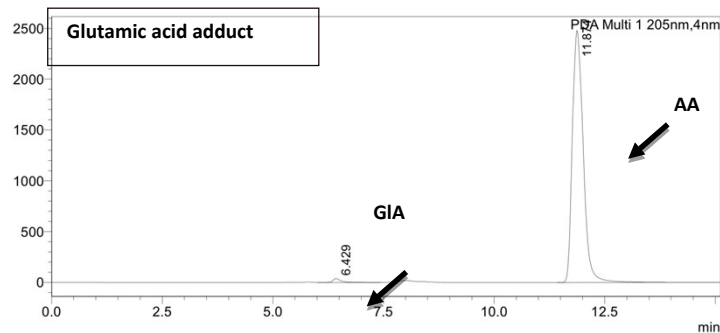
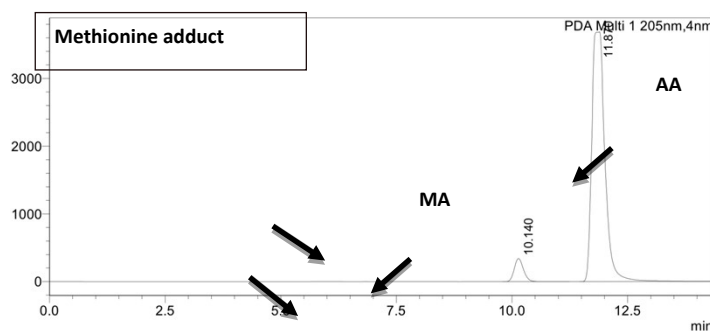
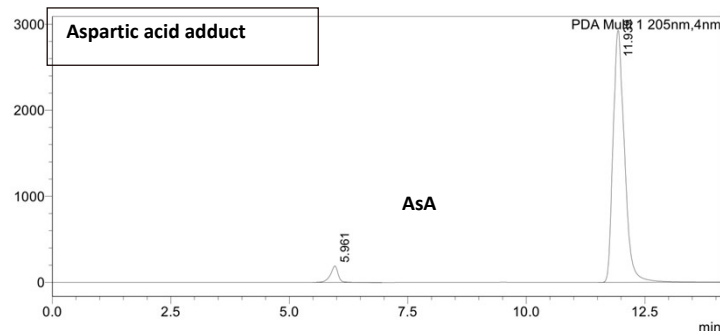
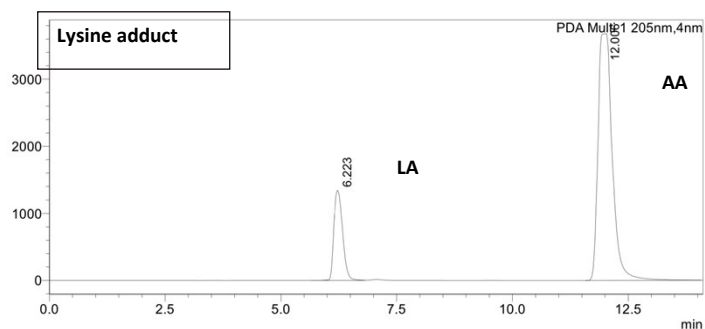
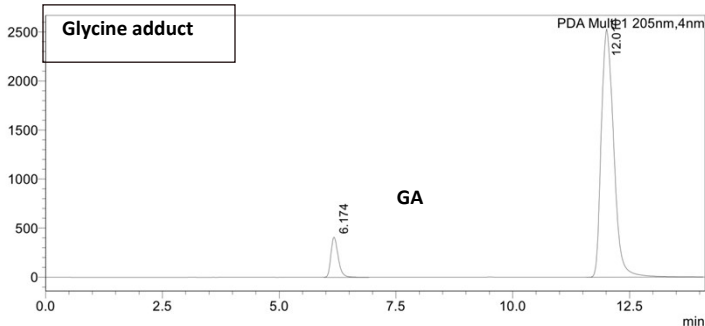
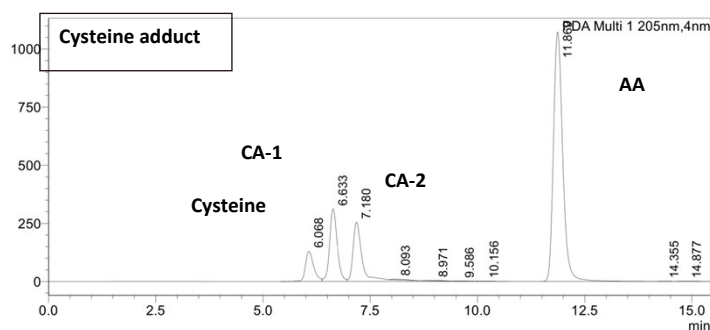
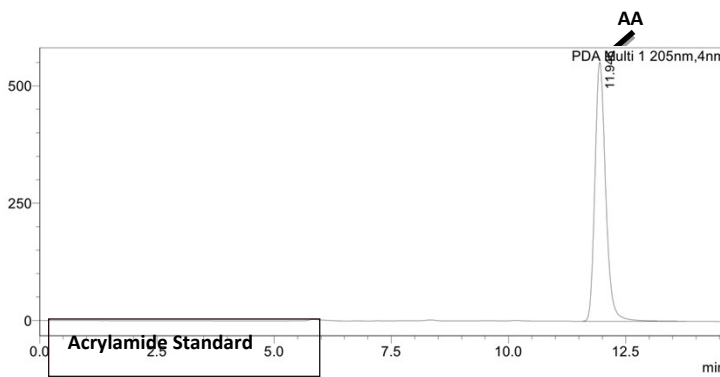
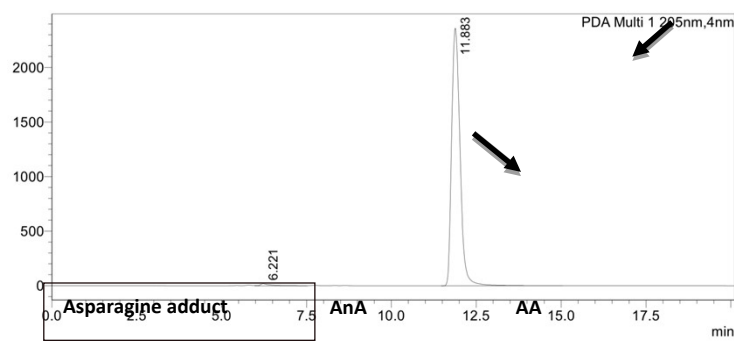


Figure S1. HPLC chromatograms for reaction products of different amino acids with acrylamide, after incubation at 80 °C for 120 min.



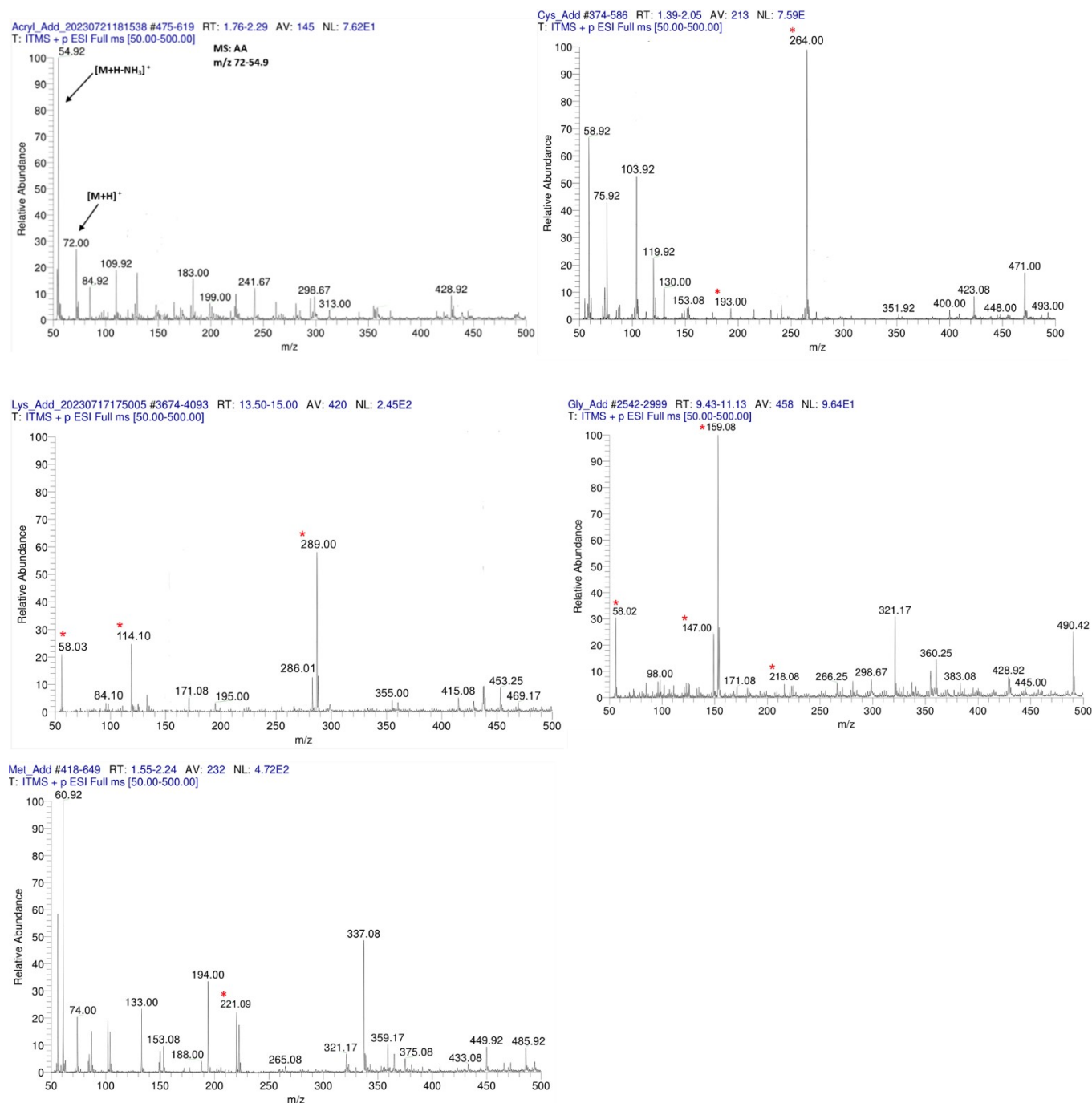


Figure S2. ESI-MS for reaction products of different amino acids with acrylamide, after incubation at 80 °C for 120 min.

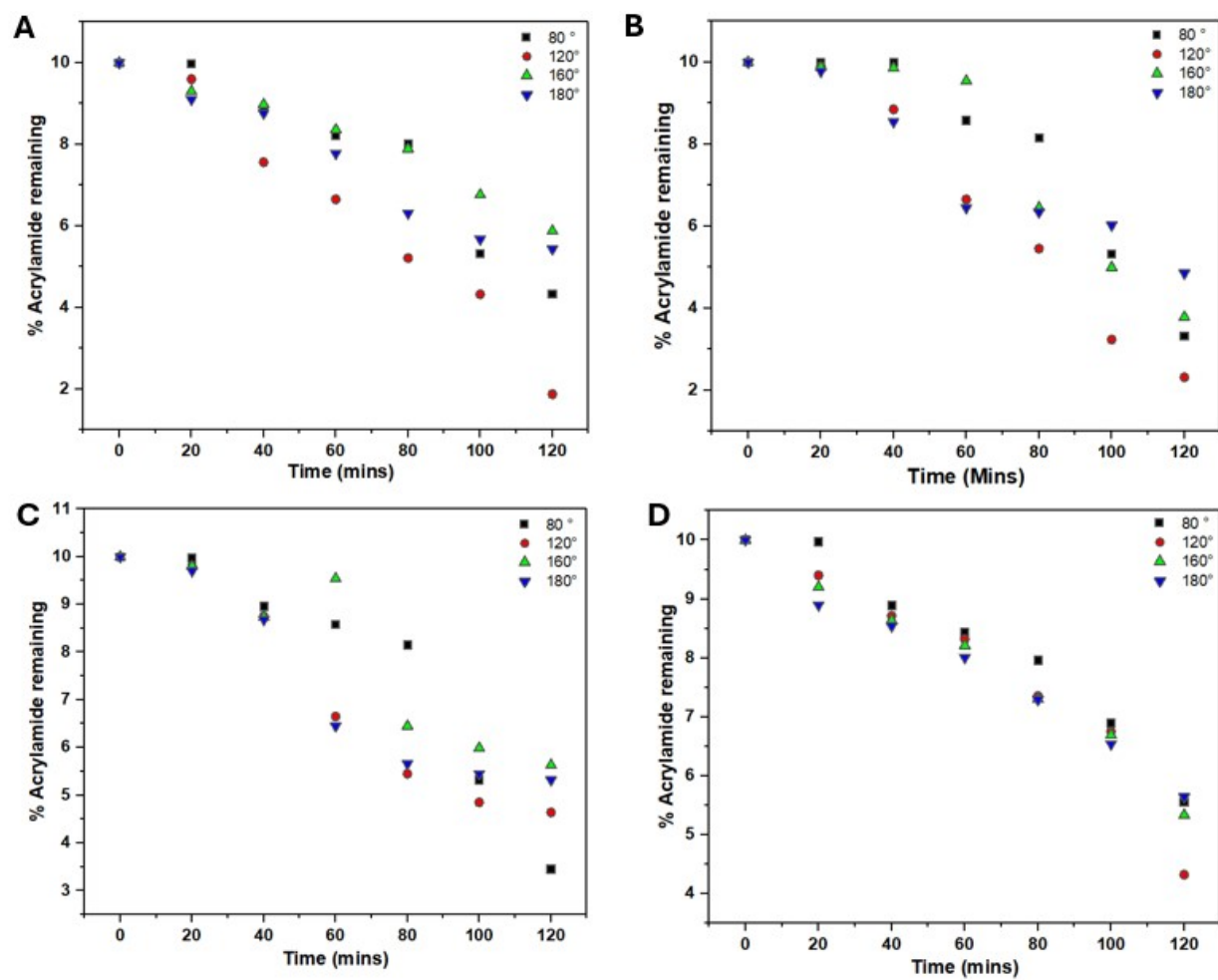


Figure S3. Effect of temperature and time of incubation on acrylamide (10 mM) remaining after reaction with amino acids (A) Cys (60 mM), (B) Lys (50 mM), (C) Gly (40 mM) and (D) Met (50 mM).

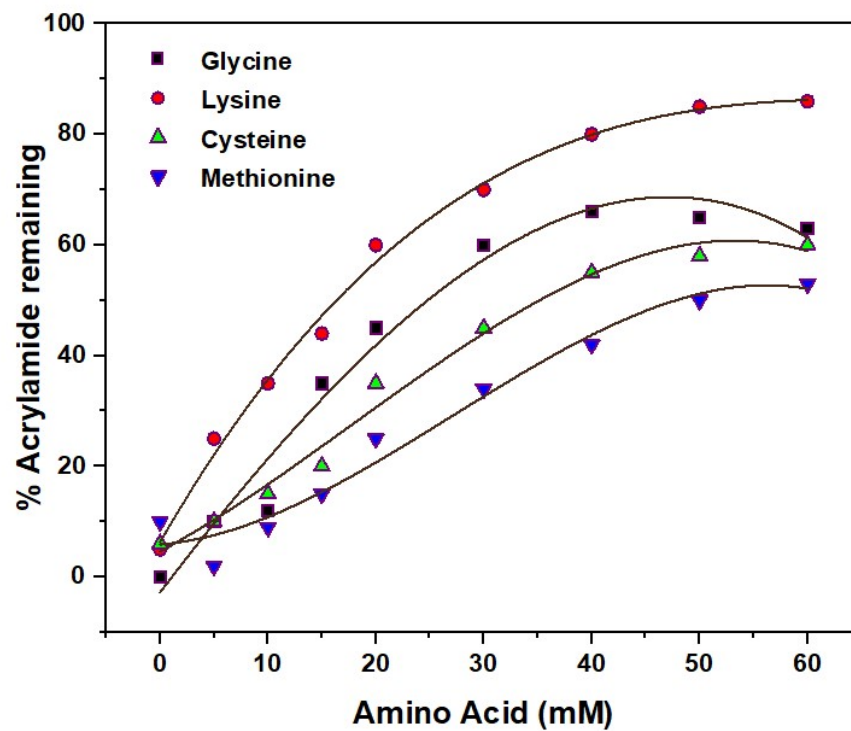


Figure S4. Effect of variation of amino acid concentration on acrylamide remaining after incubation with the amino acids, Glycine (■), Lysine (●), Cysteine (▲) and Methionine (▼), with acrylamide (10 mM) at 80 °C for 120 mins.

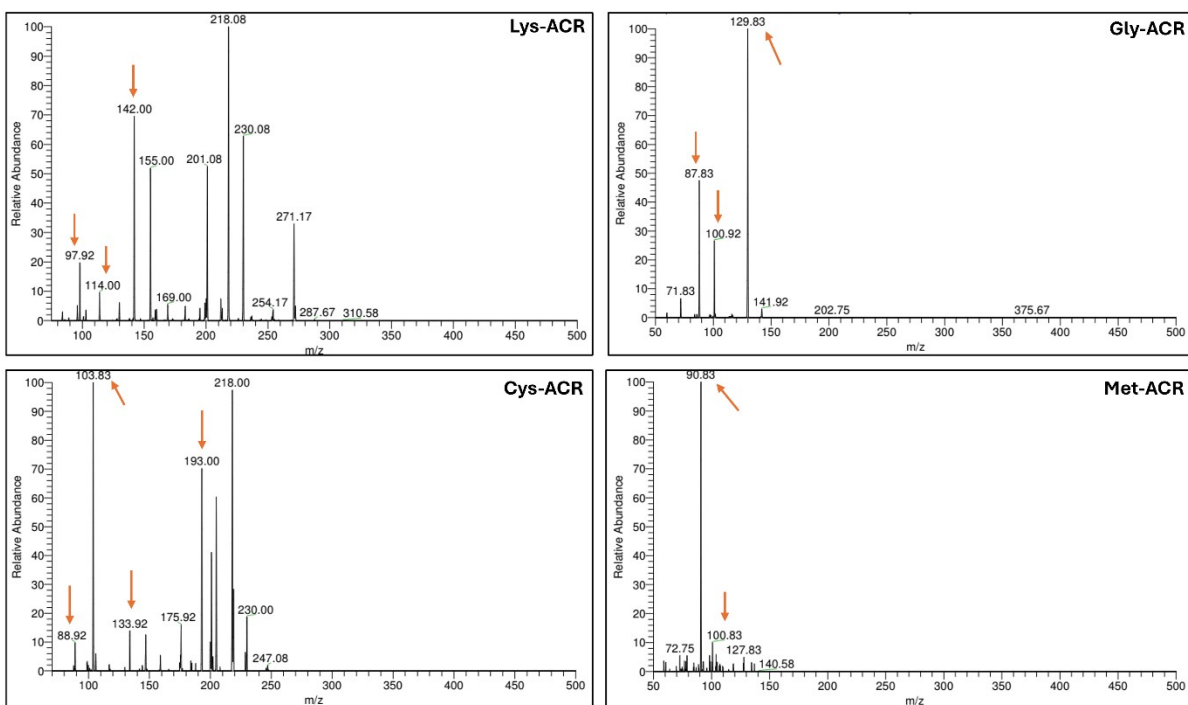


Figure S5. MS/MS performed on Lys-AA ($m/z = 289$) Gly-AA ($m/z = 218$), Cys-AA ($m/z = 264$), Met-AA ($m/z = 221$). Prominent fragment ions of AA-ACR adducts are indicated by arrows.

Table S4. MS/MS fragment ions observed for Lys-ACR-AA (m/z 289), Gly-ACR-AA (m/z 218), Cys-ACR-AA (m/z 264), and Met-ACR-AA (m/z 221) adducts.

Adduct	Precursor Ion (m/z)	Observed Fragment Ions (m/z)	Fragment Attribution
Lys-ACR	289.10	97.92, 114.00, 142.00, 218.08	Fragmentation of Lysine adduct, loss of side chains, ring formation.
		155.00, 169.00, 201.08, 230.08	Cleavage of alkyl/amide bonds in acrylamide lysine adduct.
		254.17, 271.17, 287.67, 310.58	Further loss of functional groups, product ion formation.
Gly-ACR	218.10	87.83, 100.92, 129.83	Fragmentation of glycine, loss of neutral fragments.
		71.83, 141.92	Cleavage at amide bond, formation of product ions.
Cys-ACR	264.00	88.92, 103.83, 133.92, 175.92	Loss of small functional groups from cysteine acrylamide adduct.
		193.00, 218.00, 230.00	Fragmentation at the side chain of cysteine adduct.
		247.08	Further loss of sulfur-containing group.
Met-ACR	221.09	90.83, 100.83, 127.83, 140.58	Fragmentation of methionine adduct cleavage of sulfur and alkyl groups.
		72.75	Smaller fragments from product ions of Met-ACR

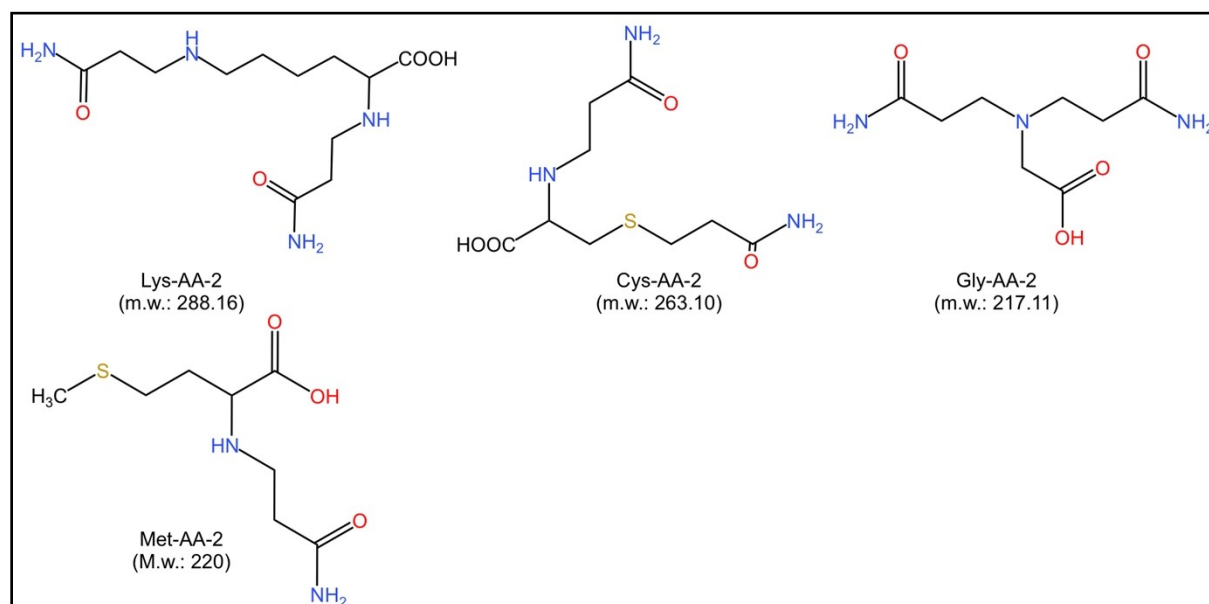


Figure S6. Structure of adducts formed by acrylamide with amino acids Lys, Gly, Cys and Met.

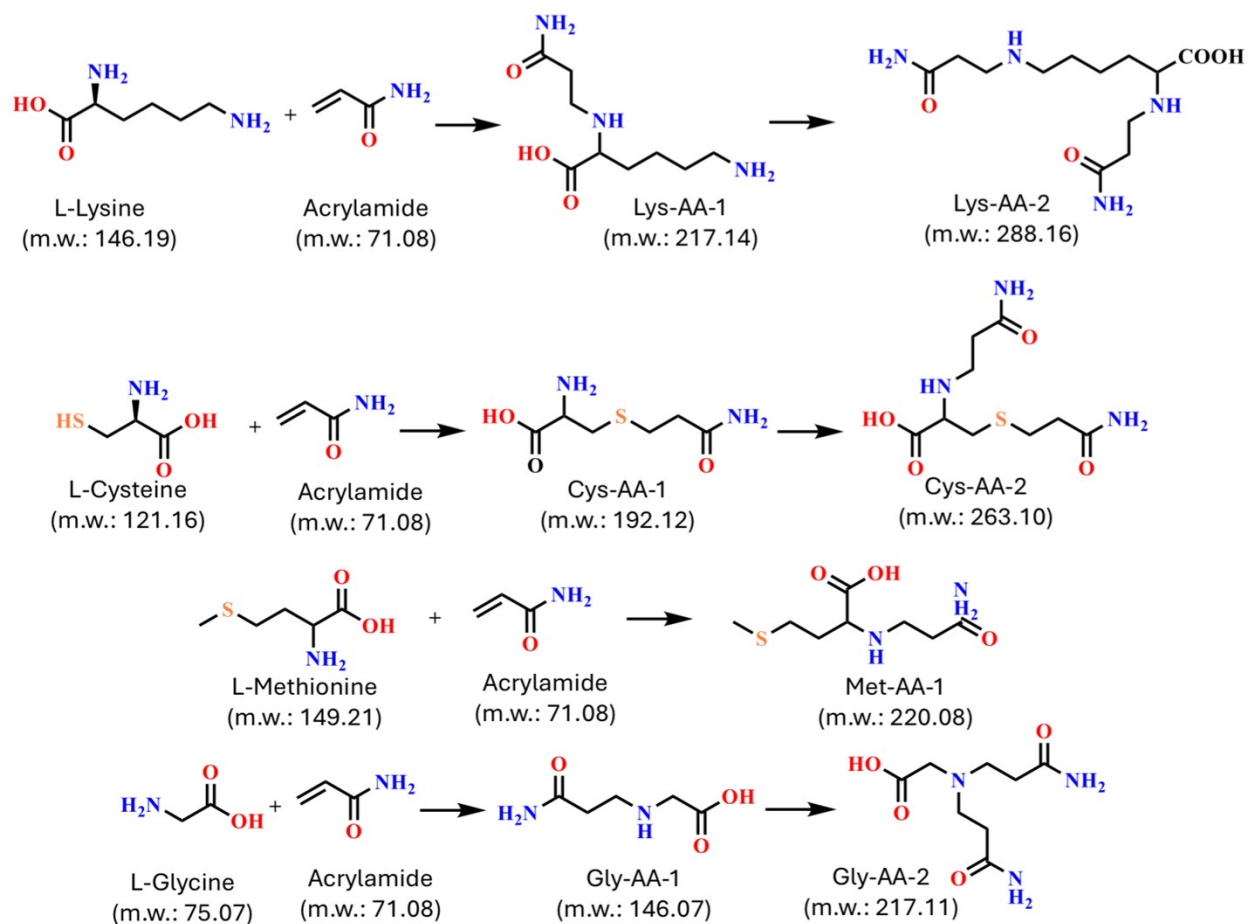
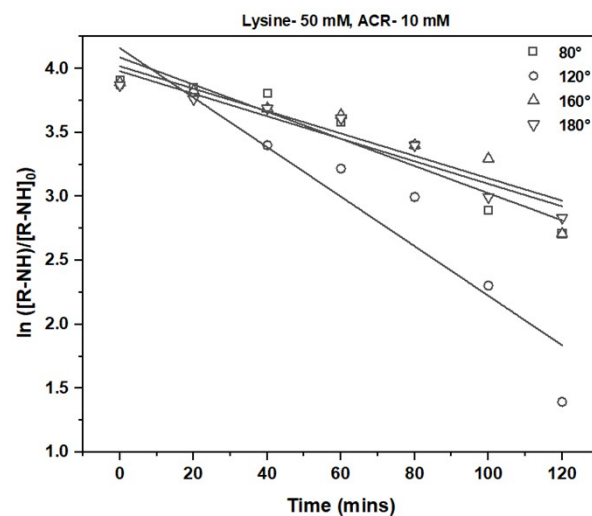
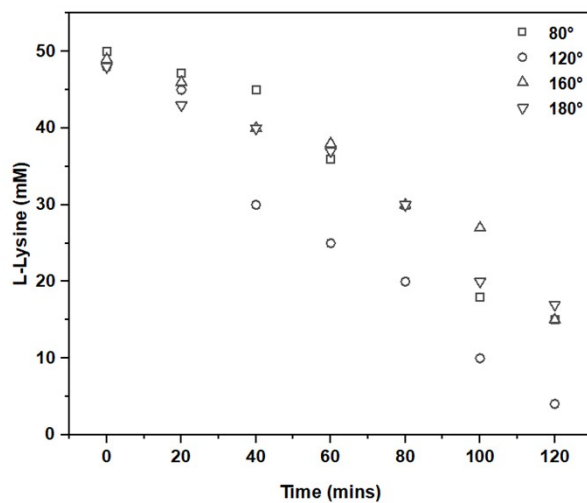
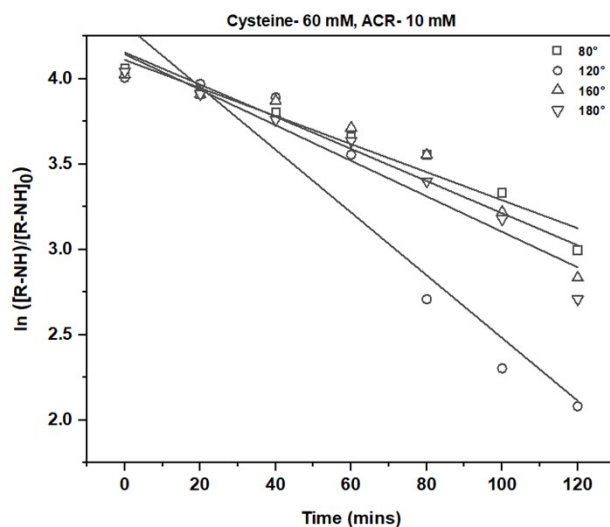
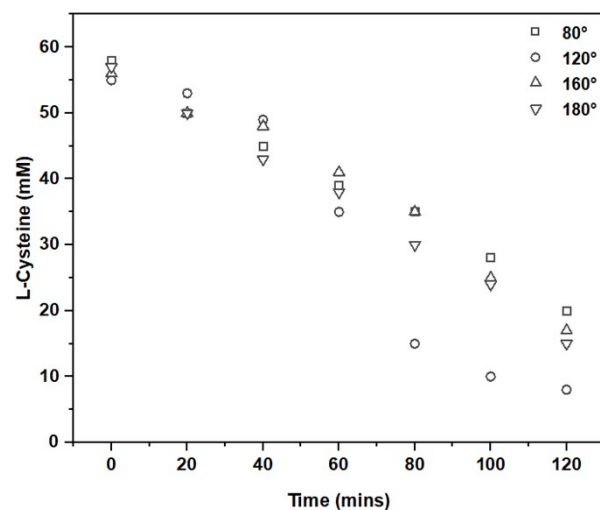
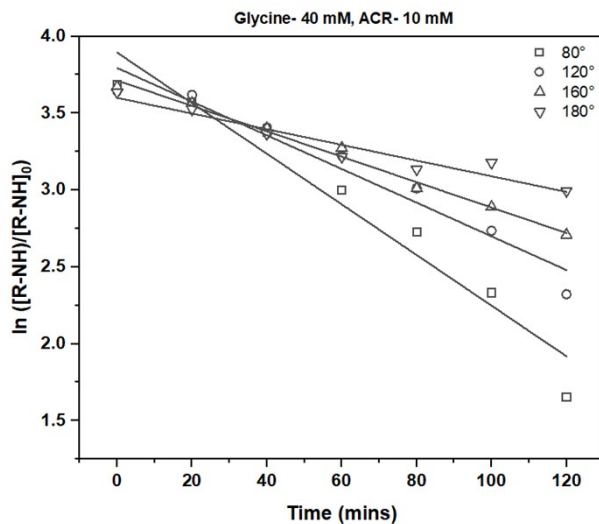
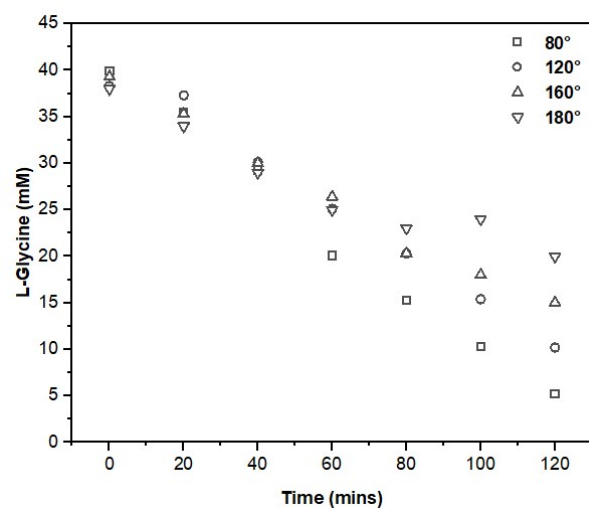


Figure S7. Prospective structures of adducts formed by ACR and AAs



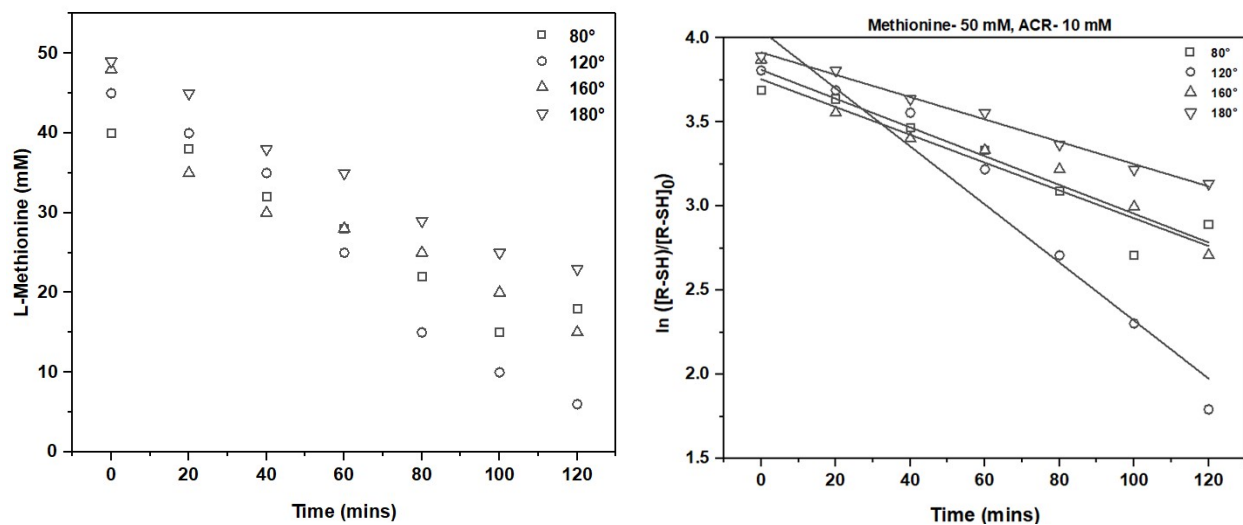
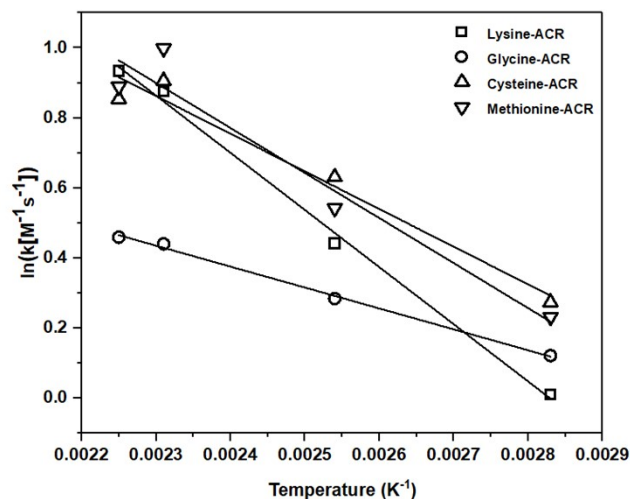


Figure S8. Reaction kinetics plots of Gly, Lys, Cys, Met with ACR at optimised pH and different temperatures at 80 (□), 120 (○), 160 (△) and 180 (▽) °C.



Activation energies calculated using Arrhenius plot equation

Lysine-ACR $Y = -1556.3x + 4.413$
Ea = 12.9 kJ/mol

Glycine-ACR $Y = -597.6x + 1.809$
Ea = 4.96 kJ/mol

Cysteine-ACR $Y = -1158.95x + 3.5608$
Ea = 9.62 kJ/mol

Methionine-ACR $Y = -1286.39x + 3.8584$
Ea = 10.69 kJ/mol

Figure S9. Arrhenius plot for the reactions of ACR with amino acids Lys, Gly, Cys and Met. The calculated activation energies (E_a) from the Arrhenius plot are presented in the table.

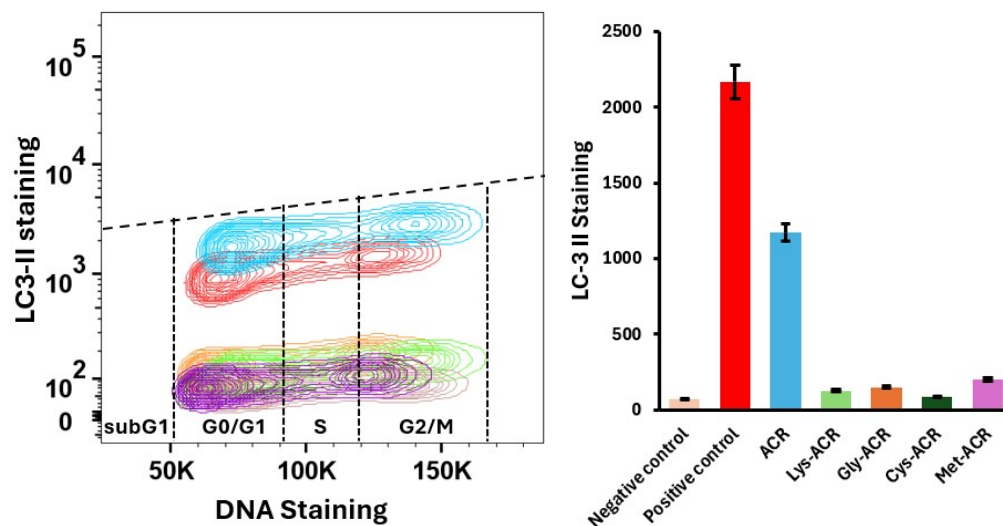


Figure S10. Autophagosome detection and formation across the cell cycle. The LC3-II expression which represents autophagosomes is plotted on y-axis in logarithmic scale, and the DNA content representing the cell cycle stages is shown on x-axis in linear scale. Vertical lines are used to distinguish among subG1, G0/G1, S, and G2/M phases of the cell cycle, and horizontal lines are placed to show upregulation of LC3-II across the cell cycle stages in response to starvation. The bar graph represents LC3-II staining levels as a marker of autophagy across different treatment groups.

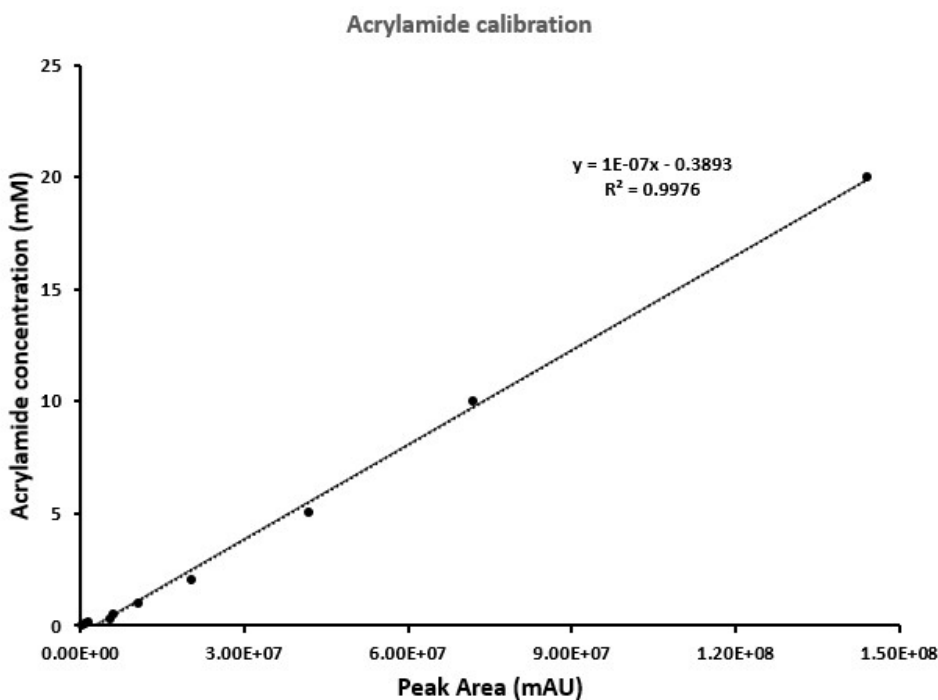


Figure S11. Calibration curve of acrylamide standard derived from HPLC method for assessment of amino acid-acrylamide products.